Applied Catalysis B: Environmental 207 (2017) 358–365

Contents lists available at ScienceDirect

Applied Catalysis B: Environmental

journal homepage: www.elsevier.com/locate/apcatb

# Nanobelt-arrayed vanadium oxide hierarchical microspheres as catalysts for selective oxidation of 5-hydroxymethylfurfural toward 2,5-diformylfuran

Yibo Yan, Kaixin Li, Jun Zhao, Weizheng Cai, Yanhui Yang*, Jong-Min Lee*

*School of Chemical and Biomedical Engineering, Nanyang Technological University, Singapore 637459, Singapore*

ARTICLE INFO

*Article history:*
Received 11 November 2016
Received in revised form 16 January 2017
Accepted 10 February 2017
Available online 14 February 2017

*Keywords:*
Nanobelt-arrayed vanadium oxide
hierarchical microspheres
Biomass
Catalytic oxidation of
5-hydroxymethylfurfural
2,5-Diformylfuran production

ABSTRACT

Nanobelt-arrayed vanadium oxide hierarchical microspheres were synthesized to catalyze selective oxidation of 5-hydroxymethylfurfural to 2,5-diformylfuran with the high conversion and selectivity of 93.7% and 95.4%, respectively. This prominent performance can be attributed to the major exposure of (010) facet with highest hydrogen adsorption capability of vanadyl group (V=O) sites and the highly oriented morphology for reactant contact and residence time control. Density functional theory calculation of the hydrogen adsorption capabilities on different facets and different chemical environmental sites has been utilized to explain the influence of different facets and lattice oxygen sites on 5-hydroxymethylfurfural oxidation performance based on hydrogen adsorption and αH-C bond cleavage steps. Isotopic studies verified the reaction mechanism and kinetic studies derived the first order reaction rate equation dependent on the 5-hydroxymethylfurfural concentration. These results suggested the crucial roles of (0 1 0) facets and the V=O sites in O-H and αH-C bonds cleavage of 5-hydroxymethylfurfural before the reduction product V-OH species further dehydrogenation by molecular oxygen.



## 1. Introduction

Biomass as a widely reproducible energy source derived from $CO_2$ fixation is drawing more attention as the alternative to limited fossil fuels. Biomass conversion into fuels and high value-add chemicals, also known as biorefinery process, occupied much effort and various methods [1–3]. 5-Hydroxymethylfurfural (HMF) generated from C6-carbonhydrates dehydration, has been expected as a crucial precursor for valuable chemicals such as 2,5-diformylfuran (DFF), 5-hydroxymethyl-2-furancarboxylic acid (HMFCA), and 2,5-furandicarboxylic acid (FDCA), among which DFF renders a most versatile intermediate transforming to numerous furan-containing functional polymers, pharmaceuticals, poly-Schiff bases, organic conductors and antifungal agents [2].

HMF oxidation to DFF encounters some challenge due to the reactive α,β-unsaturated aldehyde group on HMF. To date, selective oxidation of HMF to DFF has employed plenty of catalysts such as the manganese oxide octahedral molecular sieve [4], graphene oxide with 2,2,6,6-tetramethylpiperidin-1-oxyl (TEMPO) [2], ruthenium supported on Mg–Al hydrotalcite [5], and vanadium-based catalysts [6–8]. Among them, vanadium-containing catalysts are noticeable owing to the high selectivity toward DFF (> 90%) at low cost with unclear reaction mechanism simply comprised of the iterative redox cycles of $V^{5+}$ oxidizing HMF and $V^{4+}$ oxidized by $O_2$ [9]. Conventional $VO_x$-based catalysts are usually associated with the vanadium-heteropolyacid [1], bulk $VO_x$, and supported $VO_x$ [10]. The structure of $VO_x$ varies from monovanadate and polyvanadate with crystal structure depending on valence condition. Nevertheless, the detailed mechanism exploration and kinetic studies involving $VO_x$ physical morphology, crystalline structure and types of active sites were hardly found.

Here, we intend to synthesize a hierarchical structure of vanadium oxide nanobelt-arrayed mesoporous microsphere ($VO_x$-ms) for detailed investigation of the influence of morphology, crystalline facet, valence condition, hydrogen adsorption capabilities and adsorption convenience on catalytic performance in the selective oxidation of HMF to DFF. Structures, hydrogen adsorption capabilities on different active sites and active sites distribution are illuminated by field emission scanning electron microscopy (FESEM), transmission electron microscopy (TEM), high-resolution transmission electron microscopy (HRTEM), X-ray diffraction (XRD), X-ray photoelectron spectroscopy (XPS), Brunauer–Emmett–Teller (BET) and density functional theory (DFT) calculations.

* Corresponding authors.
*E-mail addresses:* yhyang@ntu.edu.sg (Y. Yang), jmlee@ntu.edu.sg (J.-M. Lee).

http://dx.doi.org/10.1016/j.apcatb.2017.02.035
0926-3373/

## 2. Experimental

### 2.1. Material preparation

The $VO_x$-ms utilized in this study were synthesized by solvothermal process before calcination. 0.5 mL of vanadium oxytriethoxide [$VO(OC_2H_5)_3$] was mixed with 15 mL of acetic acid in a Teflon-lined autoclave (45 mL) followed by stirring for 10 min. This sealed autoclave was located in a 200 °C oven for 1.5 h. After cooling down to room temperature, the product was centrifugated and washed several times with ethanol, then dried at 80 °C overnight. Subsequently, the $VO_x$-ms was achieved after calcination at 350 °C for 10 min (heating rate 0.5 °C $min^{-1}$) under air.

### 2.2. Characterizations

X-ray powder diffraction (XRD, GBC MMA diffractometer, Cu Kα radiation, wave length 0.15406 nm) was performed to characterize the crystalline structures. Filed-emission scanning electron microscopy (FESEM JEOL JSM-6701) was utilized to observe the morphology of materials. Transmission electron microscopy observations were conducted on a JEOL JEM 2010 200 kV TEM instrument. The specific surface area calculated by BET method was examined by the adsorption isotherms of nitrogen at −196 °C with Quantachrome Aurosorb-6B apparatus. ESCALAB 250XI photoelectron spectrometer (Thermo Fisher Scientific, USA) spectrometer and the Al Kα 1846.6 eV anode were employed to measure the XPS spectra, with C 1s peak at 284.6 eV as the reference for binding energy calibration.

### 2.3. Computational methods and models

The structure optimization and overall energy calculations were acquired by DFT code $DMol^3$ within Material Studio package of Accelerys [11]. Local density approximation together with the generalized gradient correction (GGA-PW91) was employed for the exchange-correlation functional method [12–14]. Double numerical basis set with all atoms in polarization function (DNP basis set) was performed. Vacuum thickness at 10 Å was set for periodic system to eradicate spurious interactions between adsorbate and periodic bottom-layer surface image [15]. 4.4 Å of real space cut-off was set to enhance computational performance. Self-consistent field computation set the energy tolerance as $1.0 \times 10^{-5}$ $E_h$. Energy convergence tolerance ($2.0 \times 10^{-5}$ $E_h$) and gradient convergence ($5 \times 10^{-5}$ $E_h$/A) were utilized for geometry optimization. The adsorption energy $E_{ads}$ was calculated based on: $E_{ads} = E_{(adsorbate/substrate)} - E_{adsorbate} - E_{substrate}$, where $E_{(adsorbate/substrate)}$ denoted the overall energy of adsorbate/substrate, $E_{adsorbate}$ represented merely adsorbate, and $E_{substrate}$ represented merely the substrate. More negative $E_{ads}$ indicates more stable system of adsorbate/substrate after adsorption.

### 2.4. Catalytic performance in selective oxidation of HMF

HMF oxidation reactions were performed in a Teflon-lined (25 mL) Parr high pressure reactor (Parr Instrument, USA). Typically, 1.0 mmol HMF dissolved in 10 mL ultrapure water was applied with 100 mg of catalysts, stirred at 800 rpm. The liquid phase was analyzed by high performance liquid chromatography (HPLC, Agilent 1260 Infinity) armed with UV detector (VWD, G1314B, 1260 VWD VL), refractive index detector (RID, G1362A 1260), thermostatted column compartment (TCC, G1316A), G1322A standard degasser and Bio-Rad Aminex HPX-87H, 300 mm × 7.8 mm pre-packed column using 5 mM $H_2SO_4$ as mobile phase.

### 2.5. Kinetic isotope and oxygen isotope studies

Kinetic isotope examination was carried out using deuterated HMF, including α-deuterated HMF (CHO-$C_4H_2O$-$CH_2OD$, simplified as $RCH_2OD$) and β-deuterated HMF (CHO-$C_4H_2O$-$CD_2OH$, simplified as $RCD_2OH$), as the benchmark of ordinary HMF oxidation. Oxygen isotope exchange was examined using $^{18}O_2$ to compare with $^{16}O_2$, for oxygen exchange process detection during HMF oxidation reaction.

## 3. Results and discussion

### 3.1. Characterization of $VO_x$-ms catalyst

FESEM observations displayed in Fig. 1a, b, c represented the solvothermal generation process of $VO_x$-ms precursor at 15 min, 30 min and 1.5 h respectively. The magnification image of single $VO_x$ microsphere after calcination is exhibited in Fig. 1d, with nanobelts orderly arrayed to assemble the sphere. The TEM observation in Fig. 1e verified the orderly arrayed nanobelts to form the $VO_x$ microspheres, with the lattice space of 0.41 nm characterized by HRTEM. The XRD pattern in Fig. 2a illustrated the typical $V_2O_5$ crystal structure with JCPDS card 41-1426 for both the commercial bulk $V_2O_5$ powder and the $VO_x$-ms. However, the $VO_x$-ms demonstrated the largely enhanced (0 1 0) facet signal ($2\theta = 21.7°$) than other facet signals of $VO_x$-ms, implying the majority exposure of the (0 1 0) facet. Coincidently, the (0 1 0) facet signal at 21.7° corresponded to the 0.41 nm of facet spacing according to the Bragg's Law, further verifying the HRTEM result. For characterization of the valence state of vanadium in $VO_x$-ms, XPS was performed as shown in Fig. 2b with the inset involving the V $2p_{1/2}$ and V $2p_{3/2}$ binding energy at 525 eV and 517 eV, respectively. The O 1s binding energy at 530 eV identified the $O^{2-}$ ions. Such XPS spectra are typically in accordance with the $V_2O_5$ XPS spectra [16]. Both the XRD and XPS spectra illuminated that $V_2O_5$ made the major component of $VO_x$-ms.

The growth process for this nanobelt-assembled microsphere is illustrated by Fig. 3. First, during the nucleation and aggregation step, the reaction between vanadium oxytriethoxide and acetic acid removed the $-OC_2H_5$ and formed V-O-V bond through ligand substitution:

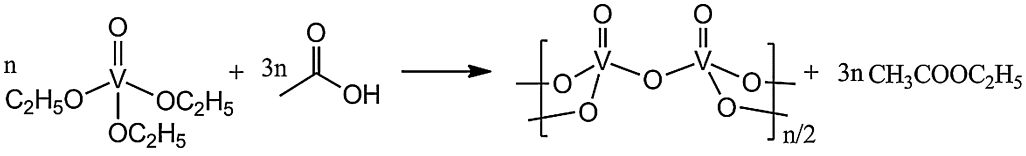


Plenty of nucleus were generated rapidly and subsequently precipitated into nanobelt-shaped nanocrystals (intermediate product solvothermally reacted for 15 min) as displayed by Fig. 1a. Second, for the surface energy minimization, these nanobelts self-assembled and orderly arrayed to form the bundles of precursor (intermediate product solvothermally reacted for 30 min) as shown in Fig. 1b. Consequently, long reaction time shaped the microsphere outline of these nanobelt-arrayed bundles, as is indicated by Fig. 1c of the product solvothermally reacted for 1.5 h. After calcination with slow heating rate, the final product $VO_x$-ms retained the morphology of the nanobelt-arrayed hierarchical microspheres. The